



**HAL**  
open science

# Robust and guaranteed output-feedback force control of piezoelectric actuator under temperature variation and input constraints

Mounir Hammouche, Philippe Lutz, Micky Rakotondrabe

## ► To cite this version:

Mounir Hammouche, Philippe Lutz, Micky Rakotondrabe. Robust and guaranteed output-feedback force control of piezoelectric actuator under temperature variation and input constraints. Asian Journal of Control, 2020, 22 (6), pp.2242-2253. 10.1002/asjc.2258 . hal-03156313

**HAL Id: hal-03156313**

**<https://hal.science/hal-03156313>**

Submitted on 2 Mar 2021

**HAL** is a multi-disciplinary open access archive for the deposit and dissemination of scientific research documents, whether they are published or not. The documents may come from teaching and research institutions in France or abroad, or from public or private research centers.

L'archive ouverte pluridisciplinaire **HAL**, est destinée au dépôt et à la diffusion de documents scientifiques de niveau recherche, publiés ou non, émanant des établissements d'enseignement et de recherche français ou étrangers, des laboratoires publics ou privés.




OATAO is an open access repository that collects the work of Toulouse researchers and makes it freely available over the web where possible

This is an author's version published in: <http://oatao.univ-toulouse.fr/27131>

**Official URL:**

<https://doi.org/10.1002/asjc.2258>

**To cite this version:**

Hammouche, Mounir and Lutz, Philippe and Rakotondrabe, Micky  *Robust and guaranteed output-feedback force control of piezoelectric actuator under temperature variation and input constraints.* (2020) Asian J Control. 2242-2253. ISSN 2242–2253

Any correspondence concerning this service should be sent to the repository administrator: [tech-oatao@listes-diff.inp-toulouse.fr](mailto:tech-oatao@listes-diff.inp-toulouse.fr)

# Robust and guaranteed output-feedback force control of piezoelectric actuator under temperature variation and input constraints

Mounir Hammouche<sup>1</sup> | Philippe Lutz<sup>1</sup> | Micky Rakotondrabe<sup>2</sup> 

<sup>1</sup>FEMTO-ST Institute, Université Bourgogne Franche-Comté/CNRS/ENSMM, Besançon, France

<sup>2</sup>LGP laboratory, ENIT / Toulouse INP, Tarbes, France

## Correspondence

Micky Rakotondrabe, FEMTO-ST Institute, Université Bourgogne Franche-Comté/CNRS/ENSMM, Besançon France.  
Email: mrakoton@femto-st.fr

## Abstract

This paper addresses the control of manipulation force in a piezoelectric tube actuator (piezotube) subjected to temperature variation and input constraints. To handle this problem a robust output-feedback design is proposed using an interval state-space model, which permits consideration of the parameter uncertainties caused by temperature variation. The design method is robust in the sense that the eigenvalues of the interval system are designed to be clustered inside desired regions. For that, an algorithm based on Set Inversion Via Interval Analysis (SIVIA) combined with interval eigenvalues computation is proposed. This recursive SIVIA-based algorithm allows to approximate with subpaving the set solutions of the feedback gain  $[K]$  that satisfy the inclusion of the eigenvalues of the closed-loop system in the desired region, while at the same time ensuring the control inputs amplitude is bounded by specified saturation. The effectiveness of the control strategy is illustrated by experiments on a real piezotube of which the environmental temperature is varied.

## KEYWORDS

input constraint, interval models, piezoelectric tube actuator, robust output-feedback, set inversion via interval analysis

## 1 | INTRODUCTION

Piezoelectric actuators, such as a piezoelectric tube and piezoelectric multimorph cantilever, are among the most used actuator in micro/nano-scales applications, particularly in micro/nano manipulation, Scanning Probe Microscopy (SPM), and Atomic Force Microscopy (AFM) due to their high speed (large bandwidth up to 1kHz), high precision (sub-nanometric), high resolution, and multi-degrees of freedom [1–6]. Unfortunately, they are characterized by nonlinearities (hysteresis, time varying parameters, creep, etc). They are also sensitive to the envi-

ronment and especially to ambient temperature variation [7]. Actually, there are several sources that may cause this thermal variation during experimentation: the lamps used to illuminate the tasks at the microscale and related cameras, the heating of the surrounding devices (voltage amplifiers...), and all other natural sources. This temperature variation considerably impacts the approximated model of the actuator and induces the change in its dynamics and its steady-state behavior. Furthermore, in micro/nano manipulation, the manipulated object is usually so fragile that if the desired performance (overshoot and rapidity) is not sufficiently respected under

this temperature variation, the manipulated object may be damaged, which makes the control of these systems not a trivial task.

Nonlinear controller design for piezoelectric actuators gained much research interest in recent decades. In these approaches, the piezoelectric actuators are approximated by uncertain nonlinear models. For instance, in [8], a nonlinear approach based on the Lyapunov function to analyze stability has been proposed. A variety of nonlinear control design based on adaptive techniques are proposed in the literature [9–11]. Moreover, there are also some predictive approaches, such as the work presented in [12,13]. Further, Sliding Mode Control (SMC) design has been widely used in the literature to control piezoelectric actuators because it provides robust performances and because it has lower computational costs [14–17]. In these approaches, the hysteresis is usually divided into a linear part and a bounded time-varying unknown part. This bounded part is considered as structured uncertainties and is overcompensated in the control law. Other approaches based on an adaptive sliding mode controller are proposed in [17–19]. Robust control techniques have also been developed when the models of the piezoelectric actuators are linear with uncertainties [20–22]. For instance, in [23,24], interval techniques have been used to derive a transfer function model with uncertainties and to design robust interval controllers for a piezoelectric actuator by using the well-known Kharitonov theorem [25]. The main advantage of this approach is the fact that parametric uncertainties could be easily modeled by bounding them with intervals [23,26–28]. However, the approach used transfer function representation and therefore was not adapted to multivariable systems. As an extension to multivariable, in this paper, a state-space based interval modeling is studied and the design of a robust controller using the state/output-feedback is developed.

The robust state-feedback controller synthesis for interval state-space models has been considered in several works [29–31]. Indeed, the concept of robust controller design for interval systems is based on placing the eigenvalues in a specific region rather than choosing an exact assignment. Among the previous works that deal with interval feedback control is the method discussed in [32], which offers a solution for this problem without using interval arithmetics. However, they are limited to systems with state and input matrices of special structures [29]. Notwithstanding, the numerous interval models with state and input matrices of standard structures have led to the necessary use of interval arithmetics and computation. Many works have been conducted in this direction. For instance [29,33] are based on the properties of non-standard interval arithmetic and a simple formulae

for regulator synthesis while [29,31] are based on the interval Ackermann's equation, the inner solutions of which are known to represent robust stabilizing controllers. Furthermore, an analytical method using matrix minors and its characteristic equation is introduced in [30]. Actually, the above works are focused on placing all the coefficients of the system's closed-loop characteristic polynomial within a desired closed-loop interval characteristic polynomial. However, only the degree of stability of the closed-loop system with state-feedback was addressed and no performance measure was discussed.

On the other hand, piezoelectric actuators are usually subjected to input constraints due to their physical limitations. These limitations must be considered during the design of a guaranteed controller in order to avoid the actuators damage additionally to the guarantee of the stability and of the desired performances. However, according to the best of our knowledge, the guaranteed control problem for interval system subjected to input constraints has received very little attention in the literature. In fact, in the last decade there are some approaches reformulating the input constraints as a convex optimization problem with Linear Matrix Inequality (LMI) constraints under some assumptions [34–36] but these methods contain a lot of parameters to set which make them not practical.

This paper provides a simple algorithm to find the range of the robust and guaranteed feedback gains to control the manipulation force of piezoelectric tube actuators subjected to input constraints and temperature variation. Such temperature variation induces variation in the model parameters. Foremost, we propose describing the impact of the temperature variation on the piezoelectric tube actuator by interval state-space model. However since measuring all states of such actuators is very difficult [37], we restrict the analysis to robust output-feedback design, which has not been addressed in previous works that deal with interval systems. The proposed approach consists in extending the poles assignment techniques into interval poles assignment techniques. Additionally, we propose converting the problem of input constraints into the inclusion problem and solve it using interval analysis.

The paper is organized as follows. Section 2 is dedicated to brief preliminaries on intervals analysis and interval matrices theory including eigenvalues computation. Section 3 presents a description of the proposed approach to synthesize the robust and guaranteed output-feedback controller itself. An application of the proposed method to control the manipulation force of a piezoelectric tube actuator is discussed in Section 4. The experimental results and verification are presented in the same section. Finally, the conclusion is in Section 5.

## 2 | INTERVAL ANALYSIS AND MATRIX THEORY PRELIMINARIES

An interval number  $\mathbf{x} = [\underline{x}, \bar{x}]$ ,  $\mathbf{x} \in \mathbb{R}$ , can be defined by the set of  $x \in \mathbb{R}$  such that  $\underline{x} \leq x \leq \bar{x}$ . In this paper the standardized notations in [38] for interval analysis are used, in which an interval number is denoted by bold font and sometimes by Lie brackets. The lower and upper bounds of an interval will be denoted by underline and overline letters respectively. Let us consider two intervals  $[x] = \mathbf{x} = [\underline{x}, \bar{x}]$  and  $[y] = \mathbf{y} = [\underline{y}, \bar{y}]$ . The result of the algebraic operations  $\diamond \in \{+, -, \cdot, /$  between these two intervals is an interval that envelopes all possible solution:

$$[x] \diamond [y] = \{x \diamond y | x \in [x], y \in [y]\} \quad (1)$$

An interval matrix is a matrix that contains at least one interval element [30]. Usually an interval matrix is defined as follow:

$$\mathbf{A} := [\underline{A}, \bar{A}] = \{A \in \mathbb{R}^{n \times n}; \underline{A} \leq A \leq \bar{A}\} \quad (2)$$

where  $\underline{A}, \bar{A} \in \mathbb{R}^{n \times n}$  and  $\underline{A} \leq \bar{A}$ . The interval matrix is characterized by its midpoint  $A_c$  and its radius  $A_\Delta$ :

$$A_c := \frac{1}{2} (\underline{A} + \bar{A}), \quad A_\Delta := \frac{1}{2} (\underline{A} - \bar{A}) \quad (3)$$

### 2.1 | Eigenvalue computation

The interval eigenvalue of  $\mathbf{A}$  is the set  $\Lambda(\mathbf{A})$  such that [30],

$$\Lambda(\mathbf{A}) = \{\lambda + i\mu | \exists A \in \mathbf{A}, \exists x \neq 0 : Ax = (\lambda + i\mu)x\} \quad (4)$$

for all  $A \in \mathbf{A}$ .

A real symmetric interval matrices  $\mathbf{A}^S$  corresponding to the interval matrix  $\mathbf{A}$  is defined as the family of all symmetric matrices denoted  $A^s$  in  $\mathbf{A}$ , that is,

$$\mathbf{A}^S = \{A^s \in \mathbf{A}\} \quad (5)$$

The real symmetric interval matrix  $\mathbf{A}^S \in \mathbb{R}^{n \times n}$  has  $n$  real interval eigenvalues. Its  $i^{\text{th}}$  eigenvalue is given by:

$$\lambda_i(\mathbf{A}^S) = [\underline{\lambda}_i(\mathbf{A}^S), \bar{\lambda}_i(\mathbf{A}^S)] := \{\lambda_i(A) | A \in \mathbf{A}^S\} \quad i = 1, \dots, n \quad (6)$$

The recent advances on interval analysis computation give the opportunity to calculate the interval eigenvalue of interval matrices. In fact, the interval eigenvalue computation does not provide an exact values for all eigenvalues of the interval matrix, however, it provides an estimation of an envelope with a box or polygonal shape that bounds all the eigenvalues of the interval matrix. For example, [39] and [40] proposed exact bounds that embrace all the eigenvalues of the symmetric interval matrices. These approaches are based on hard assumptions, which are not easy to verify [41]. Moreover, in [42], the authors proposed an approach to estimate the interval eigenvalue of real and complex interval matrices using Taylor expansion.

On the other side, [43] employed perturbation theory to make the estimation. A non-complex formula to estimate the interval eigenvalue is proposed by Rohn's in [44] for a class of symmetric interval matrices. This latter formula is extended by Hladík's to generalized interval matrices in [41]. Finally, another method to compute the interval eigenvalue of a generalized interval matrix called 'vertex approach' can be found in [45,46]. The approach is based on the computation of the characteristic equations of all edges of the interval matrix, then a convex hull function is used to estimate the outer bound of the interval eigenvalue. This method is relatively time consuming. However it provides valuable results, especially in the case of interval matrices with large numbers where the previous methods lead to overestimation most of the time.

## 3 | ROBUST CONTROL DESIGN USING INTERVAL ANALYSIS

In this paper we will adopt the classical output feedback structure to design a robust controller using interval analysis.

### 3.1 | The new structure of output feedback using interval analysis

Output-feedback control design is among the most studied in control engineering [47]. Indeed it is much simpler to implement relative to state-feedback because very few sensors are required. The main objective of output-feedback is to seek a feedback gain  $K$  such that the closed-loop system satisfies some desired performance. Such problem comes back to finding a feedback gain  $K$  that assigns the eigenvalues of the closed-loop system in a desired location within the complex plane.

Let us consider a linear Multi Input Multi Output (MIMO) system under uncertainties that are described by the following interval state-space model:

$$\begin{cases} \dot{x}(t) = \mathbf{A}x(t) + \mathbf{B}u(t) ; \\ y(t) = \mathbf{C}x(t) + \mathbf{D}u(t) \end{cases} \quad (7)$$

where  $x \in \mathbb{R}^n$ ,  $u \in \mathbb{R}^m$ ,  $y \in \mathbb{R}^p$ ,  $\mathbf{A} \in \mathbb{R}^{n \times n}$ ,  $\mathbf{B} \in \mathbb{R}^{n \times m}$ ,  $\mathbf{C} \in \mathbb{R}^{p \times n}$ , and  $\mathbf{D} \in \mathbb{R}^{p \times m}$ . The interval matrices  $\mathbf{A}$ ,  $\mathbf{B}$ ,  $\mathbf{C}$ ,  $\mathbf{D}$  are unknown but bounded by elements lying in known upper and lower bound; that is,  $\mathbf{A} = [\underline{A}, \bar{A}]$ ,  $\mathbf{B} = [\underline{B}, \bar{B}]$ ,  $\mathbf{C} = [\underline{C}, \bar{C}]$ , and  $\mathbf{D} = [\underline{D}, \bar{D}]$ . It is worth noting that the real system is non-interval but is assumed to have behavior inside the above interval model. For this matter, we maintain the signals  $x$  and  $y$  (and  $u$ ) as non-intervals. [29] The pair  $(\mathbf{A}, \mathbf{B})$  is controllable for any system matrices  $A \in \mathbf{A}$  and  $B \in \mathbf{B}$  if the controllability matrix

$$\mathbf{Y} = [\mathbf{B}, \mathbf{A} * \mathbf{B}, \dots, \mathbf{A}^{n-1} * \mathbf{B}] \quad (8)$$

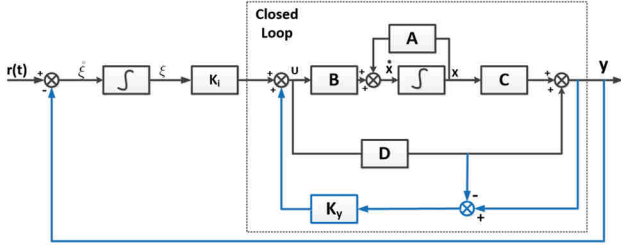


**FIGURE 1** Output-feedback with integral compensator [Colour figure can be viewed at [wileyonlinelibrary.com](http://wileyonlinelibrary.com)]

satisfies the condition

$$0 \notin \text{Det}[Y] \quad (9)$$

Let us assume that the interval system with the pair  $A, B$  is controllable. In this paper, we adopt the output-feedback control design with integral compensator to synthesize a robust controller for the interval model [48]. The integral compensator is used here instead of the static feedforward gain (DC-gain) to nullify the steady-state error in the presence of system uncertainties. The proposed control schema is shown in Figure 1 and given by:

$$u(t) = K_y(y - D \cdot u(t)) + \xi(t)K_i \quad (10)$$

where  $K_y$  and  $K_i$  are the output-feedback gain and the integral gain respectively,  $\xi(t)$  is the integral of the tracking error (i.e.,  $\dot{\xi} = r(t) - y(t)$ ,  $r(t)$  being the reference input)

The output-feedback controller with the integral compensator may be presented by a  $(n + 1)$  dimensional augmented state vector containing the state vector  $x(t)$  and the integrator state  $\xi(t)$ . The augmented system is given by:

$$\begin{aligned} \begin{pmatrix} \dot{x}(t) \\ \dot{\xi}(t) \end{pmatrix} &= \underbrace{\begin{pmatrix} (A + BK_y C) & BK_i \\ -(C + DK_y C) & -DK_i \end{pmatrix}}_{[A_c]} \begin{pmatrix} x(t) \\ \xi(t) \end{pmatrix} \\ &+ \underbrace{\begin{pmatrix} 0 \\ I \end{pmatrix}}_{[B_c]} r(t) \\ y(t) &= \underbrace{\begin{pmatrix} (C + DK_y C) & DK_i \end{pmatrix}}_{[C_c]} \begin{pmatrix} x(t) \\ \xi(t) \end{pmatrix} \end{aligned} \quad (11)$$

### 3.2 | Problem formulation

The problem of a robust and guaranteed output-feedback control for the control schema in Figure 1 can be outlined by:

1. - finding the matrix gain  $[K]$  (with  $[K] = [[K_y] [K_i]]$ ) that assigns the system eigenvalues to a desired region in the complex plane under system uncertainties that are described by interval model. The desired region in the complex plane is defined relative to the desired performance of the closed-loop system including the settling time, overshoot, and so on.

**TABLE 1** The proposed recursive SIVIA-based algorithm to seek for a set of robust gains

<p><b>SIVIA (in: <math>[A], [B], [C], [D], [K]</math> = <math>[initialbox], [k_{in}] = \emptyset, [K_{out}] = \emptyset, [K_{unfeasible}] = \emptyset, [K_{guaranteed}] = \emptyset, \epsilon, Y = \Omega_{DesiredregionofEigenvalue}</math>)</b></p>	
Step 1	Iteration $i$ - Calculate $A_c([A], [B], [C], [D], [K])$ - Calculate $eig([A_c])$ using eigenvalue computation
step 2	-If $eig([A_c]) \subseteq Y$ Then $[k_{in}] = [k_{in}] \cup [K]$ Go to step 6
Step 3	-If $eig([A_c]) \cap Y = \emptyset$ Then $[k_{unf}] = [k_{unf}] \cup [K]$ Go to step 6
Step 4	-If $[K] < \epsilon$ Then $[k_{out}] = [k_{out}] \cup [K]$ Go to step 6
Step 5	- Else bisect $[K]$ and stack the two resulting boxes.
Step 6	-If the stack is not empty, then unstack into $[K](i + 1)$ , increment $i$ and go to Step 1. -Else End.

2. - taking into account the input constraints of the system in such a way that the control input will not exceed predefined amplitudes.

In this paper we propose to use the interval analysis to handle these two problems. For this matter, we propose to reformulate the problem as follows.

**Problem:** find the set of gains  $[K]$  of the closed-loop system such that the following inclusions are satisfied:

$$\begin{cases} \mathbf{u}^*([A], [B], [C], [D], [K]) \subseteq [U_s, \overline{U}_s] \\ eig[A_c([A], [B], [C], [D], [K])] \subseteq \Omega_{Desired\ region} \end{cases} \quad (12)$$

where  $[A_c]$  is the augmented closed-loop state matrix of the system (11),  $\Omega_{Desired\ region}$  is the desired subregion of eigenvalues,  $\mathbf{u}^*$  is the control input of the interval system. which will be detailed in the following subsection, and  $[U_s, \overline{U}_s]$  are the lower and upper bounds of the control input magnitude that refers to the physical limitation of the actuator. They are constant and correspond to the maximal and minimal voltages that we can apply to the actuator.

### 3.3 | Finding the set of gains that satisfy the pole assignment specifications

In this subsection, the process of searching for a set of robust gains is transformed into a set inversion problem. Solving this latter problem permits finding the gains that assign the interval eigenvalue in the desired region.

A set inversion operation consists of searching the reciprocal image called subpaving of a compact set. In our case, in order to solve this set inversion problem, we consider the Set Inversion Via Interval analysis (SIVIA) algorithm introduced in [38], which we propose to modify. We call the

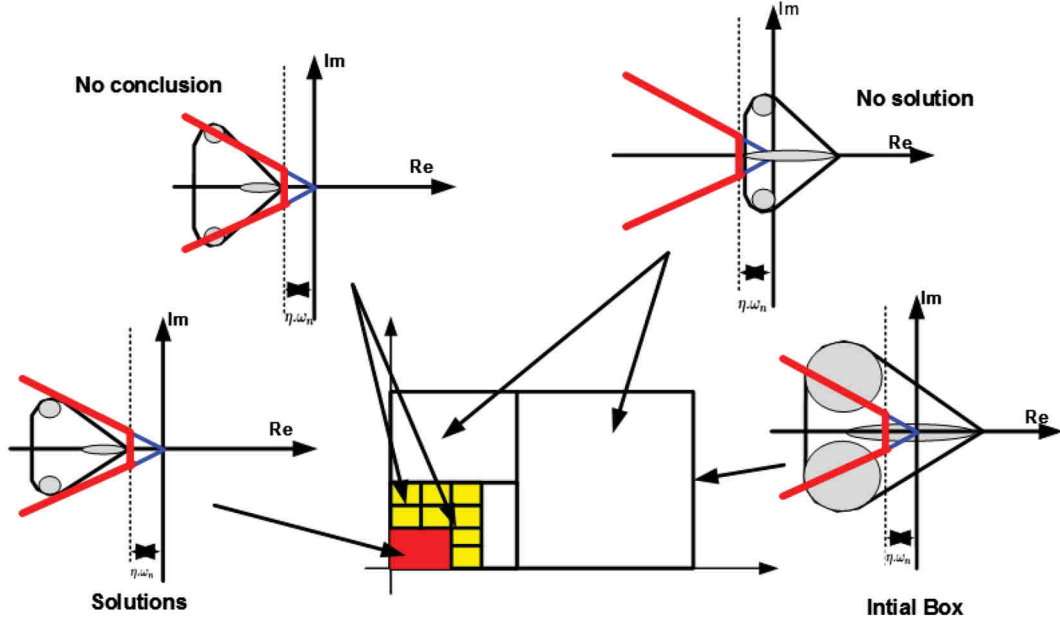


**FIGURE 2** Recursive SIVIA-based algorithm with interval eigenvalues computation [Colour figure can be viewed at [wileyonlinelibrary.com](http://wileyonlinelibrary.com)]

suggested modified algorithm the recursive SIVIA-based algorithm. In this recursive SIVIA-based algorithm, the aim is to approximate with subpaving the set solutions  $[K]$  that satisfy the inclusions (12).

The recursive SIVIA-based algorithm is outlined in Table 1 and depicted in Figure 2. To use this algorithm, we need to define an initial box  $[K_0]$  that may contain the solutions. Moreover, we should have as well the interval state-space matrices, the desired region of eigenvalues (specifications), and the accuracy for the paving  $\epsilon$ . Since the closed-loop matrix of our system is non-symmetrical, we are obliged to use the Hladík formula [41] or the vertex approach [46] in the proposed SIVIA-based algorithm to calculate the interval eigenvalue. The proposed algorithm provides a complete information about the ranges of the feedback gains including: inner (solution), outer (undefined), and unfeasible (no solution) subpavings where all the sets' subpavings were initially empty. The inner solution is the set of gains that ensure all the eigenvalues of the interval system are inside the desired region, whereas, the outer solution is the set of gains that guarantee that the inclusion condition is not satisfied. Finally, the unfeasible solution is the border set where we do not have any conclusion.

### 3.4 | Finding the set of gains that satisfy the control input constraints

All physical systems should generally operate within bounds on the control input in order to avoid overpowering of the actuators because otherwise they may be damaged. It is therefore essential to consider these limitations, called

input constraints, during the controller design. In this subsection we will convert the problem of input constraints into the inclusion problem by using the interval analysis technique [38]. Foremost, to streamline the notation let us start by redefining the closed-loop system (11) as described by equations (3.4):

$$\begin{aligned} \begin{pmatrix} \dot{x}(t) \\ \dot{\xi}(t) \end{pmatrix} &= (A^* + B^* K^* C^*) \begin{pmatrix} x(t) \\ \xi(t) \end{pmatrix} + \begin{pmatrix} 0_{n \times m} \\ I_{m \times m} \end{pmatrix} r(t) \\ \dot{X}(t) &= A_c X(t) + B_c r(t) \\ y(t) &= (C^* + D^* K^* C^*) \begin{pmatrix} x(t) \\ \xi(t) \end{pmatrix} \end{aligned} \quad (13)$$

$C_c$

such that

$$\begin{aligned} A^* &= \begin{pmatrix} A & 0_{n \times p} \\ -C & 0_{p \times p} \end{pmatrix}; \quad B^* = \begin{pmatrix} B \\ -D \end{pmatrix}; \quad C^* = \begin{pmatrix} C & 0_{p \times m} \\ 0_{m \times n} & I_{m \times m} \end{pmatrix}; \\ K^* &= (k_y \ k_i); \quad D^* = \begin{pmatrix} D \\ 0_{p \times m} \end{pmatrix}; \end{aligned}$$

The control input (10) can be reformulated as follows:

$$\begin{aligned} (I + k_y D) u(t) &= k_y C_c \begin{pmatrix} x(t) \\ \xi(t) \end{pmatrix} + \xi(t) K_i \Leftrightarrow \\ u(t) &= (I + K^* D^*)^{-1} K^* (C_c^t \ B_c)^t X(t) \end{aligned} \quad (14)$$

Since the closed-loop system will be asymptotically stable for acceptable design, the maximum of the control input is observed when the derivative of the control input is equal to zero (i.e.,  $\dot{u} = 0$ ). Thus,

$$\begin{aligned} \dot{u} &= (I + K^* D^*)^{-1} K^* (C_c^t \ B_c)^t \dot{X}(t) = 0 \Leftrightarrow \\ \dot{u} &= (I + K^* D^*)^{-1} K^* (C_c^t \ B_c)^t (A_c X(t)^* + B_c r(t)) = 0 \end{aligned} \quad (15)$$

For  $(I + \mathbf{K}^* \mathbf{D}^*)^{-1} \mathbf{K}^* (\mathbf{C}_c^t \mathbf{B}_c)^t = \Xi$  and  $\mathbf{A}_c$  are non-singular matrices (i.e.,  $0 \notin \Xi, \mathbf{A}_c$ ), we have:

$$\mathbf{X}^*(t) = -\mathbf{A}_c^{-1} \mathbf{B}_c r(t) \quad (16)$$

The condition on non-singularity of  $\mathbf{A}_c$  can be easily satisfied using an eigenvalues assignment technique in which all the eigenvalues of the interval closed-loop matrix  $\mathbf{A}_c$  can be assigned to be strictly negative.

In certain applications of piezoelectric actuators, such as in micro/nano manipulation, the input force reference is always a step or a sequence of steps signal. Hence we assume  $r$  as constant reference or constant within an interval described by  $r \in [r, \bar{r}]$ . Actually piezoelectric actuators have a badly damped step response. Therefore in closed-loop, the input control is also oscillating in order to compensate for the system's oscillation. The idea here is to find the interval that embraces all possible values of the maximum input control when the reference trajectory takes a value inside the range  $[r, \bar{r}]$ . The interval (the lower and upper bounds) of the input control can be calculated easily using the following interval computation.

With the help of equations (14) and (16) we derive the formula of the control input  $\mathbf{u}^*$  for the interval system (17):

$$\mathbf{u}^* = (I + \mathbf{K}^* \mathbf{D}^*)^{-1} \mathbf{K}^* (\mathbf{C}_c^t \mathbf{B}_c)^t (-\mathbf{A}_c^{-1} \mathbf{B}_c r) \quad (17)$$

The interval formula of the input constraint (17) is used to convert the problem of inputs constraint to inclusion problem (18) that can be solved easily using the inversion algorithms as explained in the following subsection.

$$\mathbf{u}^*([A], [B], [C], [D], [K]) \equiv [\underline{u}, \bar{u}] \subseteq [\underline{U}, \bar{U}] \quad (18)$$

### 3.5 | Summary of the search of a robust and guaranteed gains

In this subsection, the overall framework to find the set of gains that are robust and, at the same time that guarantee the input constraint is provided. The overall framework is depicted in Figure 3. The search for a set of robust and guaranteed gains is done in cascade as shown in the diagram of Figure 3. In practice, this can be done by adding the inclusion equation of the input constraint (18) in the second line of "step 2" of the recursive SIVIA-based algorithm (Table 1).

Furthermore, if one is only interested in finding the set of robust gains without input constraints, the searching process is stopped after the recursive SIVIA-based algorithm as shown in the diagram of Figure 3.

**Remark.** To search for the set of guaranteed gains that satisfy the input constraints, we should first verify the poles assignment specification to be sure that the closed-loop matrix  $\mathbf{A}_c$  is non-singular as needed in (17). Therefore, the interval control input inclusion (18) is checked only inside the solution boxes  $[K_{in}]$  that sat-

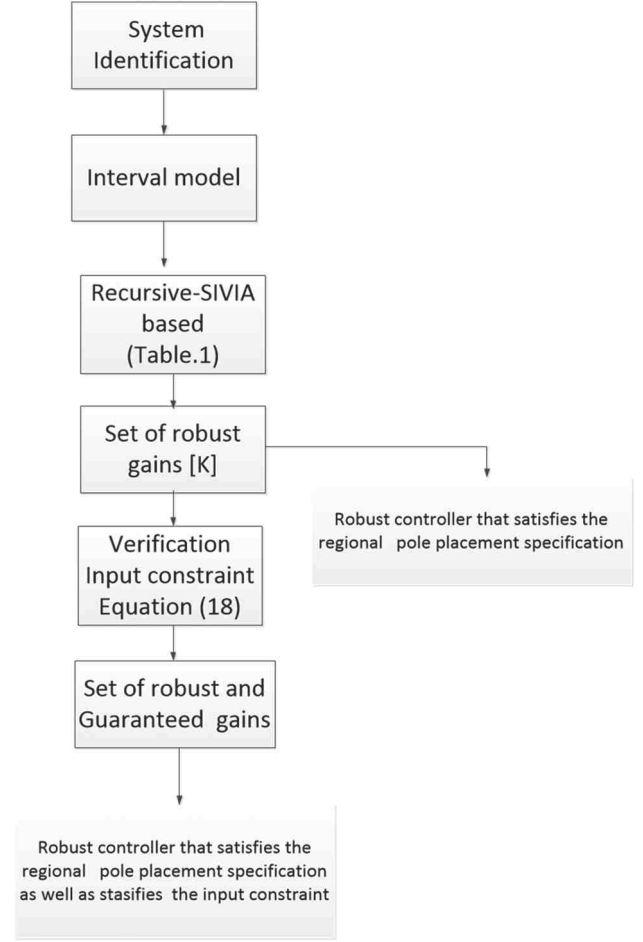


**FIGURE 3** Overall framework to obtain the set of robust and guaranteed gains [Colour figure can be viewed at [wileyonlinelibrary.com](http://wileyonlinelibrary.com)]

isfy the eigenvalues inclusion (12) where the closed-loop eigenvalues are certainly inside the desired region.

## 4 | APPLICATION TO PIEZOELECTRIC TUBE ACTUATORS

In this paper we apply the proposed modeling and control technique to a piezoelectric tube actuator. An application of this actuator is the manipulation of miniaturized objects, see Figure 4. Such manipulation application (micromanipulation) requires micrometric precision and millisecond of response time. Unfortunately, the manipulator (the actuator) is often in an environment where the temperature could vary due to the surrounding experimental setup (camera lamp, devices,...) or to other natural sources [1]. The aim of this section is to use the proposed recursive SIVIA-based algorithm to find the robust and guaranteed controller gains to further control the manipulation force of the piezoelectric tube under these thermal variation conditions.



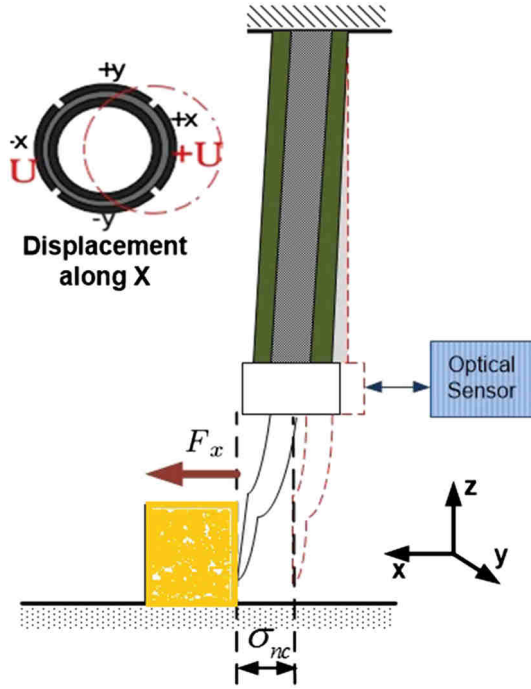


**FIGURE 4** The use of piezoelectric tube actuator to manipulate a micro-object [Colour figure can be viewed at [wileyonlinelibrary.com](http://wileyonlinelibrary.com)]

#### 4.1 | Experimental setup

The experimental setup is represented in Figure 5. It is composed of a piezoelectric tube actuator (PT230.94), an optical displacement sensors (LC2420 from Keyence company), a voltage amplifier (up to  $\pm 200V$ ), a force sensor from femtotoools-company (FT-S10000, max-10mN) and a computer with Matlab-Simulink for the implementation of the controller and for generating/acquiring the signals. A dSPACE-1103 acquisition board is used as an interface between the computer and the rest of the setup. The piezoelectric tube is made of lead-zirconate-titanate (PZT) material coated by one inner electrode (in silver) that serves as ground and four external electrodes (in copper-nickel alloy) for the electrical potentials. In addition, in order to stimulate an external variation of the ambient temperature, we use a controllable heating resistance wire around the piezoelectric actuator as shown in Figure 5 and we use a precision reference thermometer (Eurolec RT161) to measure the temperature. In this experimental part, instead of manipulating micro-objects, we manipulate the cantilever of the force sensor as shown in Figure 5.

In order to inflect the tube along the X-axis or Y-axis, we apply a potential  $+U$  on one electrode and the opposite potential  $-U$  to the counterpart electrode as depicted in Figure 6 and . Furthermore, if we apply potentials with the same sign on the four electrodes we will cause a relative displacement on the Z-axis. In the terminal of the piezo-

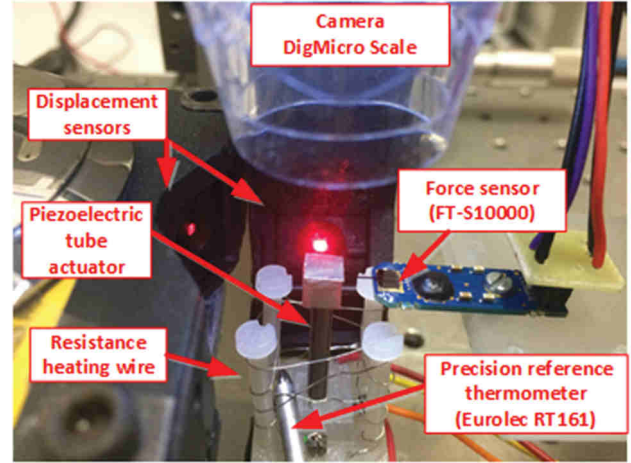


**FIGURE 5** Presentation of the experimental setup [Colour figure can be viewed at [wileyonlinelibrary.com](http://wileyonlinelibrary.com)]

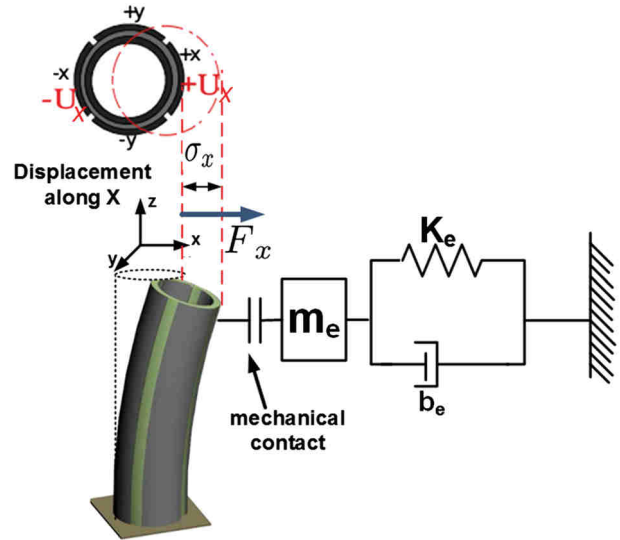


**FIGURE 6** Structure and operation of the piezoelectric tube actuator [Colour figure can be viewed at [wileyonlinelibrary.com](http://wileyonlinelibrary.com)]

electric tube, we have placed a small cube with perpendicular and flat sides to serve as reflector for the displacement sensor.

#### 4.2 | Modeling of piezoelectric tube actuator

During the experimental process we focus on the control of the manipulation force in one axis only (one degree of freedom: 1-DoF). We will note  $U_x$  the related applied voltage, and  $\sigma_x$  and  $F_x$  the resulting deflection (displacement) and the applied force to the manipulated micro-object respectively in  $x$  direction. The relation between  $U_x$ ,  $\sigma_x$  and  $F_x$  can be expressed by the linear equation in (19), whereas the sensitivity of the actuator to the temperature variation will be modeled by parametric uncertainties bounded by intervals [1].

$$\sigma_x = (d_p U_x - s_p \cdot F_x) \cdot Y(s) \quad (19)$$

where  $s_p$  and  $d_p$  are the compliance and the piezoelectric constant respectively of the piezoelectric actuator.  $Y(s)$  represents the dynamics (with  $Y(0) = 1$ ). A second order model has been chosen for the dynamic  $Y(s)$  as it includes the first resonance of the actuator and because of its simplicity [1].

The dynamics of the manipulated micro-object is represented by a second order model represented by a spring-mass-damper system with an effective mass  $m_e$ , a viscous damping coefficient  $c_e$  and a stiffness  $k_e$  as shown in Figure 6 and given by (20):

$$\sigma_x = s_0.F_x.\Psi(s) \quad (20)$$

where  $s_0$  is the micro-object compliance and  $\Psi(s)$  is its dynamics part.

Finally, after replacing the deflection in (19) with that of (20), we obtain the following linear transfer between the voltage and the force:

$$G_{xx} = \frac{F_x}{U_x} = \frac{s_p.Y(s)}{s_0.\Psi(s) + s_p.Y(s)}$$

The previous model is a *point model*, that is, the parameters are point. However, as we said before, these parameters strongly depend on the temperature evolution. The model is therefore uncertain. We suggest here to transform this model into an uncertain model where the uncertain parameters are bounded by intervals. To do that, we apply a step voltage  $U_x$  of amplitude 10 V and capture its corresponding  $F_x$  under several values of the ambient temperature varying between  $22^\circ\text{C}$  to  $29^\circ\text{C}$  with an increment of  $1^\circ\text{C}$ , as shown in Figure 7. It is worthy noting that the ambient temperature variation has an impact on the actuator as well as on the force sensor. For each step response taken at a given temperature  $T_i$  we use System Identification MatlabToolbox with Box-Jenkins method [49] to identify  $G_{xx}(T_i)$ . Note that for each temperature, the actuator is in contact with the object (the force sensor in this case). Finally, to derive the interval model  $[G_{xx}]$  of the piezoelectric actuator under temperature variation, we replace

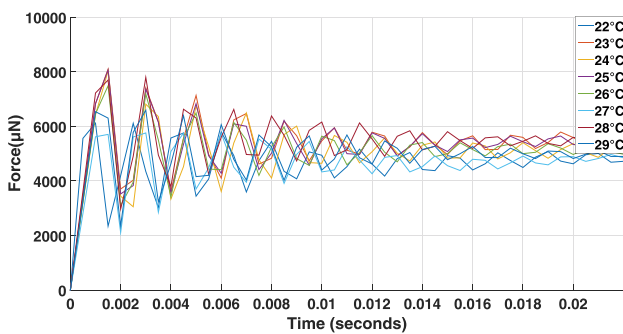


**FIGURE 7** Open-loop step response under several ambient temperatures [Colour figure can be viewed at [wileyonlinelibrary.com](http://wileyonlinelibrary.com)]

each parameter of  $G_{xx}$  by intervals as shown in (21). These intervals embrace all obtained values of each coefficient of  $G_{xx}(T_i)$  under different temperature conditions:

$$[G_{xx}](s) = \frac{[b_0]s^2 + [b_1]s + [b_2]}{s^2 + [a_1]s + [a_2]} \quad (21)$$

where

$$\begin{aligned} [b_0] &= [346.5632, 423.5774] ; & [a_1] &= [267.3284, 326.7348]; \\ [b_1] &= [6.4855, 7.9268] * 1e5; & [a_2] &= [1.2419, 1.5180] * 1e7; \\ [b_2] &= [2.7233, 3.3286] * 1e9; \end{aligned}$$

In fact, there is a compromise between the widths of the intervals parameters and the chance to find the adequate feedback controller. For example, if we augment the range of the temperature variation, larger parameter intervals are obtained, which makes the search for adequate robust gains impossible.

It is worth noting that the interval model can also be obtained under only one temperature condition, for example  $25^\circ\text{C}$ . Then, the identified parameters under this single temperature are considered as the center of the further interval parameters while the radius is imposed as 10%, see for instance [28,50]. This approach is simpler to implement than the above approach because the experimental characterization is carried out with one temperature only. However it does not guarantee that the real parameters with the various temperature will be bounded by the 10% that belong in this intervals radius.

Finally, from our interval transfer function model in (21), we derive the following state-space model in control canonical form:

$$\begin{cases} \dot{x}(t) = \mathbf{A}x(t) + \mathbf{B}u(t) \\ y(t) = \mathbf{C}x(t) + \mathbf{D}u(t) \end{cases} \quad (22)$$

$$\mathbf{A} = \begin{bmatrix} 0 & 1 \\ -[a_2] & -[a_1] \end{bmatrix}; \quad \mathbf{B} = \begin{bmatrix} 0 \\ 1 \end{bmatrix}; \quad \mathbf{D} = [b_0]$$

$$\mathbf{C} = [ [b_2] - [a_2][b_0] \quad [b_1] - [a_1][b_0] ]$$

### 4.3 | Controller calculation and experimental tests

The use of the interval model of the piezoelectric tube allows us to find a robust and guaranteed output-feedback controller that satisfies the desired performance under temperature variation. The following desired performances are adopted: negligible overshoot (1%) and with a settling time  $T_s \leq 20\text{ms}$ . We found  $\xi = \eta.\omega_n = 149.8$  and  $\theta = \sin^{-1}(\eta) = 55,7^\circ$ , where  $\eta$  and  $\omega_n$  are the damping ratio and natural pulsation respectively. Indeed, in micromanipulation and assembly applications, overshoots and oscillations are undesirable because they may cause micro/nano objects damage as well as instability in the tasks.

To calculate the set solutions  $[K]$  (with  $[K] = [[K_y] [K_i]]$ ) we use the proposed recursive SIVIA-based algorithm described in Table 1. Foremost we choose an initial box  $[K_o] = [K_y] \times [K_i] = [-10 \times 10^{-1}, 10 \times 10^{-1}] \times [-6 \times 10^{-3}, 6 \times 10^{-3}]$  and an accuracy of paving  $\epsilon = 10^{-4}$ . The choice of the initial box  $K_o$  is by trial and error. If there is no solution within a given initial box, a different box is tested. Generally the initial box has not to be too small in order to be sure we have a large enough span. Meanwhile, a too large initial box results in time-consuming problem solving. Regarding the input constraint  $U_x$ , it is supposed to be between  $[-20V, 20V]$ , and the range of the input reference is  $r \subset [-10mN, 10mN]$ .

After applying the proposed recursive SIVIA-based algorithm described, we obtain the subpaving as depicted in Figure 8. The red boxes correspond to the inner subpavings  $[K_{in}]$ , that is, the set solutions  $[K_y]$  and  $[K_i]$  that satisfy the eigenvalue inclusion (12). The white boxes correspond to the subpavings  $[K_{Unfeasible}]$  where the inclusion condition is guaranteed to be not satisfied. The yellow boxes refer to  $[K_{out}]$  where no decision on the inclusion is taken. The boxes in green correspond to the guaranteed set solution  $[K_{guaranteed}]$  in which both the inclusions condition of the eigenvalue (12) and the input constraints (18) are verified.

Actually any choice inside the solutions  $[K_{guaranteed}]$  will ensure certainly the specified performances under temperature variation and input constraints. It could be possible to choose the optimal gains that ensure the best behaviors of the closed-loop among these solutions but this is out of the scope of this paper and is a future work.

We test now the obtained solutions in simulation and in experiments. For that we select arbitrary values of controller parameters from the set solutions in Figure 8:  $K_y = -0.1 \times 10^{-3}$  and  $K_i = 0.3$ . The experimental and simulation step response for the closed-loop system are depicted in Figures 9 and 10.

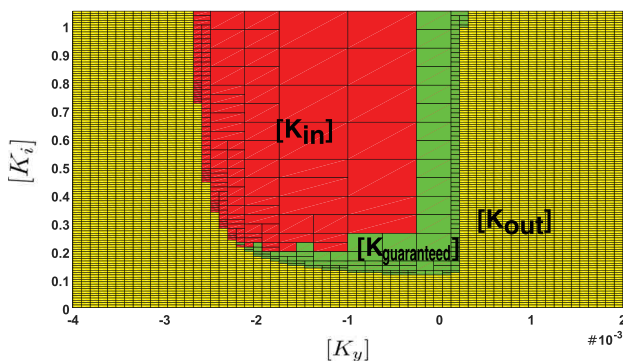


**FIGURE 8** Resulting subpaving of  $[K_y]$  and  $[K_i]$  [Colour figure can be viewed at wileyonlinelibrary.com]

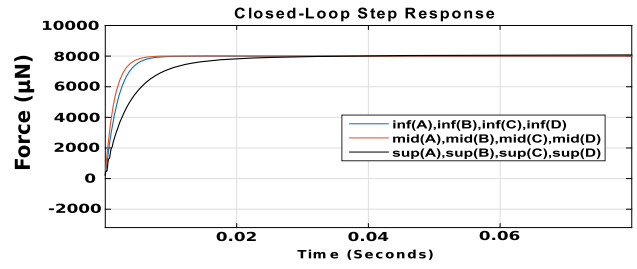


**FIGURE 9** Step response of piezoelectric tube for the closed-loop system (Simulation using Matlab) [Colour figure can be viewed at wileyonlinelibrary.com]

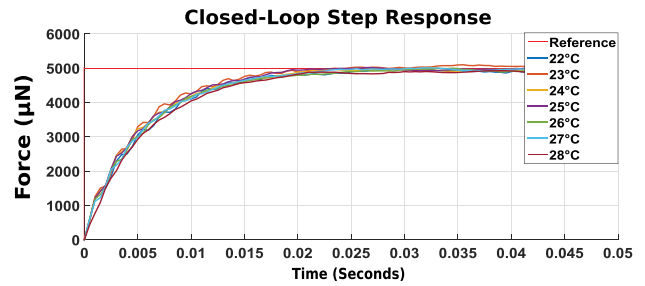


**FIGURE 10** Step response of piezoelectric tube for the closed-loop system (Experimental test) [Colour figure can be viewed at wileyonlinelibrary.com]

To perform the simulation, we take three different values of the system matrices ( $A, B, C, D$ ) inside the interval system ( $[A], [B], [C], [D]$ ): the  $\text{sup}()$ ,  $\text{inf}()$ , and  $\text{mid}()$  refer to the superior, inferior, and middle values of these interval matrices. Then the chosen controller above is applied to these *three systems*. Figure 9 displays the step response of the closed-loop system. It is clearly shown that the controller always ensures the desired performances (negligible overshoot (1%) and settling time less than 20ms) whenever the values of the matrices system ( $A, B, C, D$ ) lie inside the interval system ( $[A], [B], [C], [D]$ ).

Figure 10 represents the experimental results of the closed loop response acquired in various temperature conditions ( $22^\circ C$  to  $28^\circ C$ ). The figure also shows that the specified performances (negligible overshoot (1%) and settling time less than 20ms) are also satisfied by the closed-loop for these various temperatures.

In order to verify the locations of the closed-loop eigenvalues, we identify the closed-loop system of the experimental step responses given in Figure 10 ( $22^\circ C$  to  $28^\circ C$ ) using the Box-Jenkins method. We get second order models with eigenvalues of negligible imaginary part and a real part within the interval of  $[-3500, -170]$ . It is evident that these obtained eigenvalues of the closed-loop system are included inside the desired region ( $\text{Real}(\text{eig}([A_c])) < -\xi$ ). Indeed, we have:  $[-3500, -170] \subset ]-\infty, -\xi]$ , with  $\xi = 120$ .

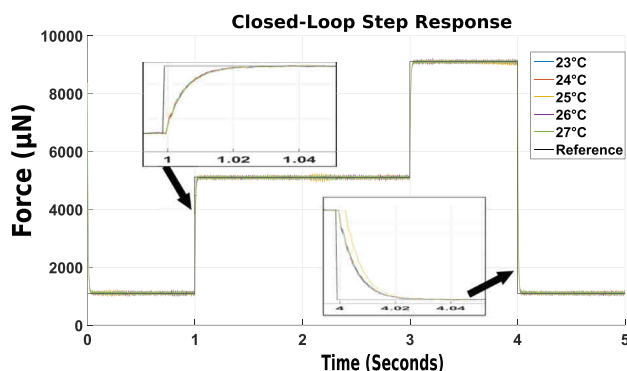


**FIGURE 11** Pursuit responses to series of steps for the closed-loop system [Colour figure can be viewed at [wileyonlinelibrary.com](http://wileyonlinelibrary.com)]

We now test the tracking performance of the closed-loop system to follow a series of steps of input reference. The result is depicted in Figure 11 where it is clearly shown that the piezoelectric tube actuator tracks successfully the desired performances.

The simulation and the experimental results presented in Figures 9, 10 and 11 show that the proposed controller provided very good performances compared with works [23,28]. Furthermore, the controllers presented in [23,28] were only tested under a fixed ambient temperature. However, in this paper the proposed controller was tested under temperature variation and input constraints.

## 5 | CONCLUSIONS

In this paper, a simple algorithm to synthesize the robust and guaranteed controller to control the manipulation force of a piezoelectric tube actuator under temperature variation and input constraint is proposed using output-feedback schema with integral compensator. The algorithm suggested to solve the problem is called a recursive SIVIA-based algorithm and is based on the combination of the Set Inversion Via Interval Analysis (SIVIA) approach, intervals eigenvalues computation, and interval input inclusion techniques. Simulation tests and experimental applications on a piezoelectric tube actuator were carried out and demonstrated the efficiency of the proposed approach.

### ORCID

Micky Rakotondrabe  <https://orcid.org/0000-0002-6413-7271>

### REFERENCES

1. M. Rakotondrabe et al., *Smart materials-based actuators at the micro/nano-scale: Characterization, control and applications*, Springer, Verlag, Berlin, 2013.

2. J.-W. Wu et al., *Adaptive tilting angles to achieve high-precision scanning of a dual probes AFM*, *Asian J. Control* **20** (2018), 1339–1351.
3. D. Habineza, M. Rakotondrabe, and Y. Le Gorrec, *Characterization, modeling and h-inf control of n-dof piezoelectric actuators: Application to a 3-dof precise positioner*, *Asian J. Control* **18** (2016), 1239–1258.
4. S. Rana, H. R. Pota, and I. R. Petersen, *A survey of methods used to control piezoelectric tube scanners in high-speed AFM imaging*, *Asian J. Control* **20** (2018), 1379–1399.
5. S. Devasia, E. Eleftheriou, and S. O. R. Moheimani, *A survey of control issues in nanopositioning*, *IEEE Trans. Control Syst. Technol.* **15** (2007), 802–823.
6. M. Rakotondrabe, *Multivariable classical prandtl-ishlinskii hysteresis modeling and compensation and sensorless control of a nonlinear 2-dof piezoactuator*, *Nonlinear Dyn* **89** (2017), 481–499.
7. D. Niederberger, *Smart Damping Materials Using shunt Control*. Zürich, Switzerland: Eidgenössische Technische Hochschule ETH Zurich, Switzerland, 2005.
8. H. Aschemann, J. Minisini, and A. Rauh, *Interval arithmetic techniques for the design of controllers for nonlinear dynamical systems with applications in mechatronics*, *J. Comput. Syst. Sci. Int.* **49** (2010), no. 5, 5–16.
9. F. Ikhouane, V. Mañosa, and J. Rodellar, *Adaptive control of a hysteretic structural system*, *Automatica* **41** (2005), 225–231.
10. X. Tan and J. S. Baras, *Adaptive identification and control of hysteresis in smart materials*, *IEEE Trans. Autom. Control* **50** (2005), 827–839.
11. J. Yao and W. Deng, *Active disturbance rejection adaptive control of uncertain nonlinear systems: Theory and application*, *Nonlinear Dyn.* **89** (2017), 1611–1624.
12. F. Lydoire and P. Poignet, *Nonlinear model predictive control via interval analysis*, *IEEE Conference on Decision and Control*, Seville, Spain, 2005, pp. 3771–3776.
13. B. J. Kubica, *Preliminary experiments with an interval model-predictive-control solver*, *Parallel Processing and Applied Mathematics*, Springer, Cham, 2016, pp. 464–473.
14. H. Ma, J. Wu, and Z. Xiong, *Pid saturation function sliding mode control for piezoelectric actuators*, *IEEE/ASME Advanced Intelligent Mechatronics*, Besacon, France, 2014, pp. 257–262.
15. J. Li and L. Yang, *Finite-time terminal sliding mode tracking control for piezoelectric actuators*, *Abs. and Appl. Anal.* **2014** (2014), 9, 760937.
16. L. Yang, Z. Li, and G. Sun, *Nano-positioning with sliding mode based control for piezoelectric actuators*, *International Conference on Mechatronics and Control*, Jinzhou, China, 2014, pp. 802–807.
17. S. F. Alem, I. Izadi, and F. Sheikholeslam, *Adaptive sliding mode control of hysteresis in piezoelectric actuator*, *International Federation of Automatic Control* **50** (2017), 15574–15579.
18. S. H. Chung and E. Fung, *Adaptive sliding mode control of piezoelectric tube actuator with hysteresis, creep and coupling effect*, *ASME International Mechanical Engineering Congress and Exposition*, Vancouver, British Columbia, Canada, 2010, pp. 419–428.
19. Y. Li and Q. Xu, *Adaptive sliding mode control with perturbation estimation and pid sliding surface for motion tracking of a piezo-driven micromanipulator*, *IEEE Trans. Control Syst. Technol.* **18** (2010), 798–810.

20. M. Rakotondrabe, Y. Haddab, and P. Lutz, *Quadrilateral modelling and robust control of a nonlinear piezoelectric cantilever*, IEEE Trans. Control Syst. Technol. **3** (2009), 528–539.
21. S. Salapaka et al., *High bandwidth nano-positioner: A robust control approach*, Rev. Sci. Inst. **73** (2002), 3232–3241.
22. G. Schitter, A. Stemmer, and F. Allgower, *Robust 2 dof-control of a piezoelectric tube scanner for high speed atomic force microscopy*, American Control Conference, Denver, CO, USA, 2003, pp. 3720–3725.
23. S. Khadraoui, M. Rakotondrabe, and P. Lutz, *Interval force/position modeling and control of a microgripper composed of two collaborative piezoelectric actuators and its automation*, Int. J. Control Autom. Syst. **12** (2014), 358–371.
24. J. Bondia et al., *Guaranteed tuning of pid controllers for parametric uncertain systems*, Conference on Decision and Control, Nassau, Bahamas, 2004, pp. 2948–2953.
25. V. L. Kharitonov, *Asymptotic stability of an equilibrium position of a family of systems of differential equations*, Differ. Equ. **14** (1978), 1483.
26. M. Rakotondrabe, *Performances inclusion for stable interval systems*, American Control Conference, San Francisco, CA, USA, 2011, pp. 4367–4372.
27. S. Khadraoui, M. Rakotondrabe, and P. Lutz, *Combining h-inf approach and interval tools to design a low order and robust controller for systems with parametric uncertainties: Application to piezoelectric actuators*, Int. J. Control **85** (2012), 251–259.
28. S. Khadraoui, M. Rakotondrabe, and P. Lutz, *Robust control for a class of interval model: Application to the force control of piezoelectric cantilevers*, IEEE Conference on Decision and Control, Atlanta, GA, USA, 2010, pp. 4257–4262.
29. Y. Smagina and I. Brewer, *Using interval arithmetic for robust state feedback design*, Syst. Control Lett. **46** (2002), 187–194.
30. B. M. Patre and P. J. Deore, *Robust state feedback for interval systems: An interval analysis approach*, Reliab. Comput. **14** (2010), 46–60.
31. M. L. M. Prado, A. Lordelo, and P. Ferreira, *Robust pole assignment by state feedback control using interval analysis*, World Congress, Prague, Czech, Brisbane, Australia, 2005, pp. 951–951.
32. K. Wei, *Stabilization of linear time-invariant interval systems via constant state feedback control*, IEEE Trans. Autom. Control **39** (1994), 22–32.
33. I. V. Dugarova. (1989). *Application of interval analysis for the design of the control systems with uncertain parameters*, Ph.D. Thesis, Tomsk State University, Russia.
34. L. Yu, Q. Han, and M. Sun, *Optimal guaranteed cost control of linear uncertain systems with input constraints*, Int. J. Control Autom. Syst. **3** (2005), 397–402.
35. L. Yu, *An lmi approach to reliable guaranteed cost control of discrete-time systems with actuator failure*, Appl. Math. Comput. **162** (2005), 1325–1331.
36. A. Al-Jiboory and G. Zhu, *Robust input covariance constraint control for uncertain polytopic systems*, Asian J. Control **18** (2015), no. 4, 1489–1500.
37. C. Clévy, M. Rakotondrabe, and N. Chaillat, *Signal measurement and estimation techniques issues in the micro/cano world*, Springer-Verlag, New York, 2011, page 978.
38. L. Jaulin, *Applied interval analysis: With examples in parameter and state estimation, robust control and robotics*, Springer Science & Business Media, Berlin, London, UK, 2001.
39. A. Deif, *The interval eigenvalue problem*, J. Appl. Math. Mech. **71** (1991), no. 1, 61–64.
40. L. Kolev and S. Petrakieva, *Assessing the stability of linear time-invariant continuous interval dynamic systems*, IEEE Trans. Autom. Control **50** (2005), 393–397.
41. M. Hladík, *Bounds on eigenvalues of real and complex interval matrices*, Appl. Math. Comput. **219** (2013), 5584–5591.
42. G. Mayer, *A unified approach to enclosure methods for eigenpairs*, J. Appl. Math. Mech. **74** (1994), 115–128.
43. H-S. Ahn, K. L. Moore, and Y. Chen, *Monotonic convergent iterative learning controller design based on interval model conversion*, IEEE Trans. Autom. Control **51** (2006), 366–371.
44. J. Rohn, *A handbook of results on interval linear problems*, Czech Academy of Sciences, 2005.
45. S. P. Bhattacharyya and L. H. Keel, *Robust control: The parametric approach*, *Advances in Control Education*, Elsevier, Pergamon, 1995, pp. 49–52.
46. M. T. Hussein, *Assessing 3-d uncertain system stability by using matlab convex hull functions*, Int. J. Adv. Comput. Sci. Appl. **2** (2011), 13–18.
47. V. Syrmos, C. Abdallah, P. Dorato, and K. Grigoriadis, *Static output feedback a survey*, Automatica **33** (1997), 125–137.
48. R. C. Dorf and R. H. Bishop, *Modern control systems*, Pearson, London, Upper Saddle River, New Jersey, 1998.
49. L. Ljung, *System identification toolbox: user's guide*, Citeseer, Natick, MA USA, 1988.
50. M. Hammouche, P. Lutz, and M. Rakotondrabe, *Robust feedback control for automated force/position control of piezoelectric tube based microgripper*, IEEE Conference on Automation Science and Engineering, Xi'an, China, 2017, pp. 598–604.

## AUTHOR BIOGRAPHIES



### **Mounir Hammouche**

received the Engineer diploma in Control Engineering from the Ex-American Institute of Boumerdes University (Algeria) in 2012, Magister degrees in Automatic Control from the Polytechnic School of Algiers (EMP) in 2014, and his master on the Technology of Information and Control (ScTIC) at the university of Paris Est Créteil (UPEC) in 2015. He obtained the PhD degree from the Université Bourgogne Franche-Comté with research affiliation at the FEMTO-ST research institute in 2018. His research interests include the multi-input/multi-output (MIMO) modeling and robust control design for uncertain systems, control design using interval analysis, optimal control, robust stability analysis and compensation of nonlinearities.



**Philippe Lutz** joined the University of Franche-Comté, Besançon, as Professor in 2002. He was the head of the research group “Automated Systems for Micromanipulation and Micro-assembly” of the AS2M department of FEMTO-ST Institute from 2005 to 2011. He was the Director of the PhD graduate school of Engineering science and Microsystems with more than 400 PhD students from 2011 to February 2017, and he is currently the head of the Doctoral College. Since January 2017, he is the director of the AS2M Research department of FEMTO-ST. His research activities at FEMTO-ST are focused on the design and control of micro-nano systems, microgrippers, micro-nano robots, feeding systems and micro-nano manipulation, assembly stations, and Optimal design and control of piezoelectrically actuated compliant structures. P. Lutz received several awards of IEEE, authored over 90 refereed publications (50 in high standard journals), serves as associate editor for the IEEE Transaction on Automation Science and Engineering and as Technical Editor for the IEEE/ASME Transactions on Mechatronic, is member of several steering committees and is member of the IEEE Robotics and Automation Society (RAS) Committee on Micro-Nano Robotics.



**Micky Rakotondrabe** (S'05-M'07) received the HDR degree in control systems from the Université de Franche-Comté, Besançon France, in 2014. He has been an Assistant Professor in 2006-2007 and then Associate Professor in 2007-August 2019 with the

Université de Franche-Comté since 2007 with research affiliation at the FEMTO Institute, France. Since Sept 2019, he is Full Professor at the National School of Engineering (ENIT), a campus of the Toulouse INP, in Tarbes France.

Dr. Rakotondrabe is or was a member of the IEEE/RAS Technical Committee (TC) on Micro/Nano Robotics and Automation and of the IFAC TC on Mechatronics. He received several recognition prizes. In 2016, he was a recipient of the Big-On-Small Award during the IEEE MARSS International Conference. This award is to recognize a young professional (<40yo) with excellent performance and international visibility in the topics of mechatronics and automation for manipulation at small scales. In 2018, he is nominee for Distinguished Lecturer of Micro/Nano Robotics & Automation at the IEEE/RAS Society. He is or was an Associate Editor or a Guest Editor in prestigious journals related to Robotics, Automation and Mechatronics (IEEE/ASME Transactions on Mechatronics, IEEE Robotics and Automation Letters, IEEE Transactions on Electronics, IFAC Mechatronics, MDPI Actuators)

**How to cite this article:** Hammoiuche M, Lutz P, Rakotondrabe M. Robust and guaranteed output-feedback force control of piezoelectric actuator under temperature variation and input constraints. *Asian J Control*. 2020;22:2242–2253. <https://doi.org/10.1002/asjc.2258>